Structure discovery for metallic glasses using stochastic quenching

E. Holmström,[1,2] N. Bock,[2] T. Peery,[2] E. Chisolm,[2] R. Lizárraga,[1,2] G. De Lorenzi-Venneri,[2] and D. Wallace[2]
[1]*Instituto de Física, Facultad de Ciencias, Universidad Austral de Chile, Casilla 567, Valdivia, Chile*
[2]*Theoretical Division, Los Alamos National Laboratory, Los Alamos, New Mexico 87545, USA*
(Received 30 April 2010; published 27 July 2010)

We investigate the distribution of local minima in the potential-energy landscape of metals. The density of energy minima is calculated for Na by using a pair-potential method to quench from stochastic configurations for system sizes ranging from 1 to 4000 atoms. We find a minimum system size, approximately 150 atoms, above which the density of energy minima is dominated by one sharp peak. As the system size is increased, the peak position converges to an asymptotic value and its width converges to zero. The findings of the pair-potential method for Na are confirmed by first-principles calculations of amorphous Al and V. Finally we present an example in which our results are applied to the complex bulk metallic glass $Zr_{52.5}Cu_{17.9}Ni_{14.6}Al_{10}Ti_5$ (Vitreloy 105). The calculated density and bulk modulus of the Vitreloy are in good agreement with experiments. The analysis presented here shows that the thermodynamic limit is better described by one large supercell calculation than by an average over many smaller supercell calculations. We argue that the minimum cell size that is needed to accurately perform such a large supercell calculation for metallic glasses is about 150 atoms.

DOI: 10.1103/PhysRevB.82.024203 PACS number(s): 61.20.Gy, 61.25.Mv, 62.20.de, 71.23.Cq

I. INTRODUCTION

An amorphous structure differs from a crystal by the lack of structural order. Many materials can be produced in the amorphous state and their properties differ considerably from the crystal. One important class of amorphous materials is the bulk metallic glasses[1,2] that show nonconventional combinations of properties such as high strength and hardness, very low magnetic anisotropy, and good corrosion resistance.[1,3–7]

One way to accurately predict such static properties from a theoretical point of view is to use first-principles density-functional theory (DFT) methods.[8,9] The problem is that, in contrast to the crystalline case, the coordinates of the atoms in the structure are unknown and there is no symmetry that can be exploited to reduce the computational effort. Hence, a crucial step in a first-principles description of an amorphous material is to find a reliable set of coordinates that describes the disordered structure. The standard way to tackle this problem is to use molecular dynamics (MD) to simulate the experimental process of melting a crystal and equilibrating the resulting liquid at some elevated temperature for a sufficiently long time, and then quenching (rapidly freezing the system) at some rate.

The MD approach is very time consuming and it means that the experimental cooling rates, that are on the order of 10^7 K/s, are out of reach. Standard cooling rates in MD calculations are on the order of 10^{12} K/s.[10,11] Additionally, in first-principles MD, only relatively small systems can be treated, usually on the order of 100 atoms. For that reason, it is desirable to find alternative, less computationally demanding methods to calculate the coordinates of the amorphous state. One possibility is to quench directly from stochastic configurations since that would remove the computationally expensive temperature equilibration part from the standard MD method. We have shown before that such an alternative way of finding amorphous structures is not only possible but also very efficient.[12] The method is motivated by the single random valley approximation (SRVA) from vibration-transit theory.[13,14] The central idea is that the potential-energy landscape (PEL) of a large number of atoms is dominated by degenerate local minima corresponding to maximally amorphous structures. By maximally amorphous it is understood that the atoms are randomly packed in a structure where there is no long-range order present and the forces on all atoms are zero. Two such structures then have, for example, the same pair-distribution functions and distributions of bond angles. Hence, from an experimental point of view, they are indistinguishable and have identical properties. This means that in the asymptotic limit when the system size becomes large, it is sufficient to find one single such random valley in the potential-energy landscape to have a good description of the amorphous structure. In Ref. 12 we demonstrated that the distributions of structural and energetic properties of amorphous configurations generated by quenching from a MD trajectory at a high temperature and quenching from stochastic configurations are the same for a Na system of 500 particles. Unfortunately, such a cell size is too large to be accessible for standard first-principles methods and calculations must hence be restricted to smaller system sizes.

In this paper, we investigate the size dependence of the distribution of local potential-energy minima obtained by stochastic quenching to determine the smallest size of the supercell where reasonable results may be expected. First we calculate this distribution for a simple monatomic system of Na atoms up to a system size of 4000 atoms using a well-tested pair potential and a model Lennard-Jones potential. We verify the trends found in Na for amorphous Al and V using a standard DFT method. Finally we perform two independent calculations of the bulk modulus of the complex bulk metallic glass $Zr_{52.5}Ti_5Cu_{17.9}Ni_{14.6}Al_{10}$ (Vitreloy 105) using 150 atom structures obtained by stochastic quenching.

II. THEORY

A. Stochastic quench procedure

The PEL is a scalar function in $3N$ dimensional configuration space of the N particle system. Hence, a N-particle system evolves on the PEL as a single point moving on the $3N$-dimensional, time-independent landscape of the many-body potential-energy surface $\Phi(\{\mathbf{r}\})$ where the set of particle coordinates $\{\mathbf{r}\}$ spans the configuration space of the material.

The assumption in the SRVA is that for large enough systems, the PEL is completely dominated by the potential-energy valleys that correspond to atomic structures without long-range order (random valleys). These structures correspond to the most random amorphous phase that is possible under the constraint that the forces on all atoms are zero. Note that this does not in any way exclude the possibility of short- or medium-range ordering. All these valleys are assumed to have the same energy at the minima and the same distributions of vibrational mode frequencies.[13] With these assumptions, all structures that are significant in the thermodynamic limit are equal and it is hence only necessary to find one such structure to have a good description of the amorphous phase.

Assuming that the PEL has the features outlined above, the fastest way to find an amorphous structure that correspond to a random valley is to quench directly from a starting configuration where the atoms are placed at random positions throughout the supercell. This does not guarantee that we find a random valley, but as we will show in the following section, the probability increases rapidly as the system size, N, becomes larger.

We use the following procedure to obtain an amorphous structure. We generate a set of N random positions within a supercell. In order to avoid numerical problems with our minimizer, we need to check the closest ion-pair distance and reject such a random guess in case the shortest pair distance is smaller than a cutoff, $r_{\mathrm{cut}}=0.2$ a.u. This reduces the effective configuration space we sample by removing a small volume which corresponds to such small pair distances. The excluded volume corresponds to ion configurations at very high potential energies.

In the case of Na, once we constructed 1000 initial random configurations for each supercell size we performed a constant-volume (41.20 Å^3/atom for both potentials) structural relaxation using the Polak-Ribiére conjugate gradient method until the potential-energy difference between iterations was less than 10^{-15} Ry/atom and ion movement was less than 10^{-6} a.u. per step.

It has been found before that different minimization methods do not introduce any bias in the distribution of local minima energies.[15] We can therefore assume that our method samples the energy distribution of the minima in the PEL in an unbiased way. As a consequence, we have obtained a temperature-independent, nonbiased energy distribution of the local minima of the potential-energy landscape. After relaxation, the average potential energy per atom Φ_0/N was saved for each of the 1000 configurations. The distributions of potential-energy minima for the starting configurations and the relaxed structures are shown in Fig. 1.

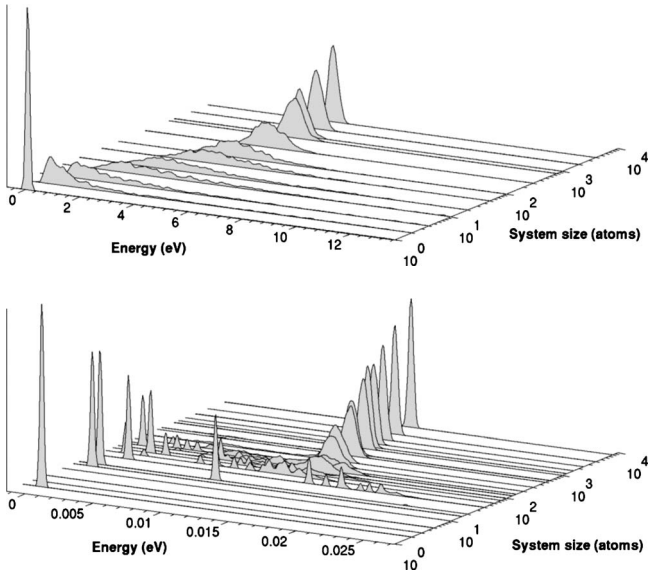

FIG. 1. (Upper panel) Total distribution of starting configuration energies as function of supercell size before quenching. (Lower panel) Total distribution of energy minima as function of supercell size after quenching. The deltalike peak at 0 eV for $N=2$ corresponds to the bcc crystal structure. The data have been broadened to construct the images. The energy scale is relative to the Na bcc crystal structure in both panels.

B. Computational methods

1. First-principles method

The first-principles calculations were performed by means of the projector augmented wave[16,17] method as implemented in the Vienna *ab initio* simulation package (VASP).[18–21] This method is based on DFT.[8,9] The exchange-correlation energy for all cases was calculated using the generalized gradient approximation with the Perdew, Burke, and Ernzerhof functional.[22]

For the Al and V calculations we used a plane-wave energy cutoff of 300 eV. The total-energy convergence criterion was set to 10^{-8} eV and the number of $\boldsymbol{k}$ points was carefully converged for every cell size so that the energy difference between $\boldsymbol{k}$-point sets was below 0.1 meV/atom.

For the Vitreloy calculation, the total-energy convergence criterion was 10^{-8} eV. In order to speed up the calculations we used the single Γ $\boldsymbol{k}$ point. This approximation is motivated by the fact that, in this case, we are calculating energy differences of comparable cell sizes and the errors due to the single $\boldsymbol{k}$-point sampling are canceled to a large extent. The total amount of quench steps for the initial structure were close to 800. The structure was first relaxed with a low-energy cutoff for the number of plane waves (205 eV) for about 700 quench steps in order to reach an approximately relaxed structure. Then the energy cutoff was increased to 342 eV until convergence (about 100 more steps).

2. Pair-potential method

The extensive quench calculations where we investigate the N dependence of the PEL are carried out for metallic Na

at the density of the liquid at melt using our model interatomic potential. This Na potential was derived in pseudopotential perturbation theory, with an added Born-Mayer repulsion, and was calibrated from experimental crystal data at zero temperature and pressure.[23] The potential has since been shown to give excellent results for a broad range of experimental properties of crystal and liquid Na, for a brief summary see Refs. 24 and 25.

To analyze the sensitivity of the results to the form of the pair potential, we also performed quenches from stochastic configurations by means of a standard Lennard-Jones potential

$$\phi(r) = \epsilon\left[\left(\frac{\sigma}{r}\right)^{12} - 2\left(\frac{\sigma}{r}\right)^{6}\right], \tag{1}$$

where $r=|\mathbf{r}_i-\mathbf{r}_j|$ is the distance between atom pairs, $\epsilon=2.044$ mRy, and $\sigma=7.85$ a.u. For both potentials, periodic boundary conditions were used and the potentials were cutoff at $r=20$ a.u. for computational efficiency.

III. RESULTS

A. Energy minima distributions

In order to analyze the effects from the periodic boundary conditions in our stochastic quench procedure, we evaluated the potential energy of our initial configurations that have randomly distributed atomic positions. In the upper panel of Fig. 1 we show the potential-energy distributions of these configurations before quenching. Since the positions of the atoms are untouched at this point, the result can only depend on the imposed periodic boundary conditions of the supercells and the small excluded volume that is determined by r_{cut}. In order to facilitate the comprehension of Fig. 1 the raw data has been broadened. We can see that there is a deltalike peak close to 0 eV when the system size is one atom. This is because the structure is then forced to be exactly single cubic due to the boundary conditions, independently of the position of the atom. Between system sizes of 2 to about 200 atoms, the energy distributions are very broad and span an energy range of about 10 eV. Above 200 atoms the distributions become narrow again and the position of the peak approaches an asymptotic value. The narrowing of the distribution here is due to the fact that the cells become large enough for the pair-distribution functions to converge to one (cf. Figs. 1–3 in Ref. 12). The total energy of the cell then becomes just an integral of the pair potential, which is the same for all cells.

In the lower panel of Fig. 1 we show the energy minima distributions after quenching from the randomly distributed positions of the configurations in the upper panel. For small system sizes $N\lesssim 20$ the distributions consist of one or a few delta peaks, some of which are off-scale in this plot. The distribution of these narrow peaks is the result of symmetric high-energy structures. For cell sizes with two atoms the quench always resulted in the bcc crystal structure which can be seen as a sharp peak at 0 eV. For cell sizes between 30 and 150 atoms the delta peaks are located at lower energies but are still spread out over a broad energy range. As the cell size is increased, one prominent peak appears and for cell sizes above 150 atoms it becomes the dominating feature of the distribution.

The appearance of this peak is understood as a property of the potential-energy landscape and not from the uniform randomness of the atomic positions as in the unquenched case in the upper panel of Fig. 1. This reinforces the assumption of the SRVA that the PEL is dominated by degenerate local energy minima.

This quenching approach was verified in Ref. 12 by comparing a distribution consisting of 1000 stochastic quenches to a distribution of energy minima as obtained by quenching 1000 structures from a MD trajectory at 800 K along a steepest decent path.[14] The system size was 500 atoms in both cases. The mean values of the distributions agreed to within 0.1 meV and the standard deviations agreed to within 0.01 meV. The accuracy of our pair potential was also confirmed in terms of total energy for $N=150$ atoms by means of a first-principles stochastic quench calculation. The total energy per atom of the first-principles calculation was compared to the total energy per atom for crystalline Na in the bcc crystal structure and the difference was 12.76 meV/atom. This was compared to the difference between the bcc structure and the peak position of the $N=150$ distribution for the Na pair potential that was 12.75 meV/atom.

To investigate how sensitive these results are to a change in the pair potential we also performed a similar set of quenches with the Na potential exchanged by the Lennard-Jones (LJ) potential [Eq. (1)] at the same density. The parameters of the LJ potential were adjusted to give similar density and energies as the Na potential, but the LJ potential has a much steeper repulsive part at short distances and a longer range attractive part at large distances. The quench results for the LJ potential are very similar to those of the Na pair potential and the main features of the energy distribution are preserved. At small system sizes the distributions are characterized by a few sharp peaks whereas for larger cell sizes (above about 100 atoms) a broader peak emerges that becomes sharper with increased cell size (data not shown).

These model potentials are both well known to be difficult to stabilize in the amorphous state. From the results above we hence conclude that model systems that are traditionally used to simulate amorphous structures such as, e.g., the binary Lennard-Jones mixture (see Ref. 26) would show a similar behavior.

B. Means

In Fig. 2 we show the mean of the distributions of the different pair-potential results together with the mean of the distribution before quenching. For the Na potential, the mean has a large value for system sizes below 20 atoms. Above 20 atoms, the mean reaches a minimum and then oscillates until about $N=100$. At about $N=150$ atoms, the mean starts to converge toward the asymptotic value although convergence to within the millielectron volt range is reached above $N=500$. A similar situation is evident in the case of LJ potentials, which is also shown in the figure. Some convergence was achieved above 20 atoms in system size but to avoid

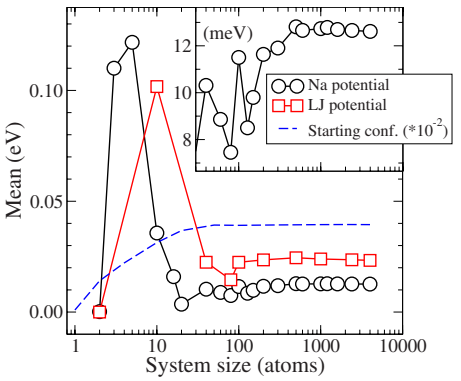

FIG. 2. (Color online) Mean value of the distributions as function of supercell size calculated by Na and LJ pair potentials. The energies are given relative to the bcc crystal structures as calculated by the respective potentials. (Inset) The mean value of the Na pair-potential results in the large N limit. Note that the scale on the x axis is the same in both plots but the y axis is labeled in millielectron volt in the inset.

large fluctuations of the mean the system size had to be larger than 100 atoms. The mean value of the starting configurations before quenching converges at about 100 atoms as well. Note that in this case the mean has been rescaled.

The potential energies are of course not universal so that other system sizes may be required in order to achieve convergence in the millielectron volt range for other materials. However, the evolution of the mean shows that, in general, there is an inherent error associated with the system size that cannot be improved by calculating averages over many small uncorrelated systems. The reason is that below the $N=150$ limit, the precursor of the asymptotic peak in the distribution is absent so that the probability to find an amorphous structure with potential energy close to the asymptotic value is extremely low.

C. Standard deviations

In Fig. 3 we show the standard deviation of the distributions as function of system size. It is important to note that the standard deviation was obtained from the raw data and not from the smeared curves in Fig. 1. In the same figure we also show the standard deviation of the subset of the data that constitutes the peak at high N. For that case the standard deviation was obtained (somewhat arbitrarily) by measuring the full width at half maximum of the peak from the smeared data and then calculating the standard deviation by assuming that the peak has a Gaussian shape. For small system sizes, the distributions consist of several delta peaks that correspond to different high-energy crystal structures. For that reason, the standard deviations do not provide useful information below $N=40$. For the rest of the system sizes we can see that the distance between the standard deviations of the peak and the full distribution is decreasing when the system size is increased. At about $N=1000$, the standard deviation of the whole distribution and the peak coincides, which simply means that all quenches resulted in amorphous structures. The results are thus in good qualitative agreement with the distributions in Refs. 27–29 obtained by MD simulations at high temperatures.

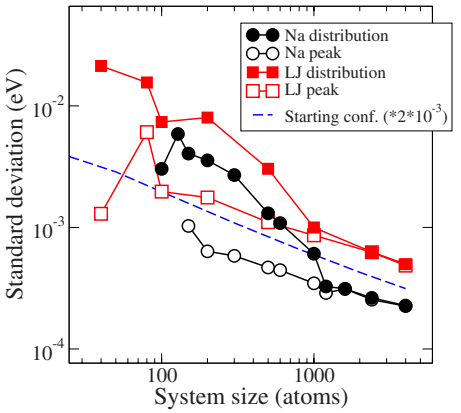

FIG. 3. (Color online) Standard deviations of the distributions of local energy minima as calculated with the LJ and Na pair potentials. Also shown is the standard deviation of the potential energy of the starting configurations before quenching.

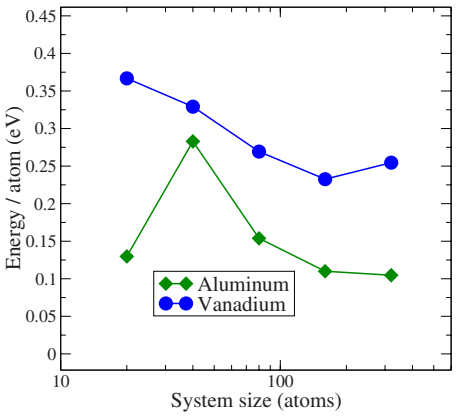

FIG. 4. (Color online) First-principles total energy per atom of amorphous Al and V systems as function of number of atoms N. The energy scale is relative to the total energy of crystalline fcc Al and bcc V, respectively.

D. First-principles calculations

1. Al and V

We have further tested the N dependence of the total energy per atom for two metallic systems, namely, Al and V by performing DFT calculations. Because the computational effort is large, we have chosen to perform one single calculation per system size. If the PEL for these metals are similar to Na, the resulting plot should have similar features as the mean values presented for Na in Fig. 2. With only one calculation per system size there is, of course, a probability that we find some crystallized or semicrystallized structures, especially for the smaller system sizes. Figure 4 displays our results. We can see that the energy per atom in both systems is converging in a similar way as for Na. The $N=160$ outlier structure of V was analyzed by observing the atomic positions graphically and it was found to be indeed partially crystallized with an indication of plane formation. This may be

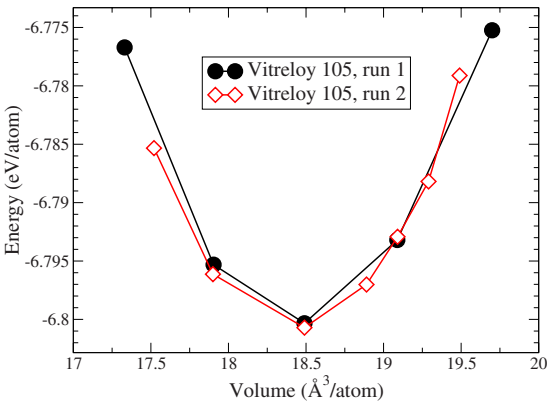

FIG. 5. (Color online) The total energy per atom for the two independent runs of $Zr_{52.5}Cu_{17.9}Ni_{14.6}Al_{10}Ti_5$ (Vitreloy 105).

seen as a slightly lower energy than expected for that point in Fig. 4.

2. Real amorphous metallic glass

The Na, V, and Al amorphous materials are examples of monoatomics systems that are difficult to realize experimentally. Therefore, we also performed two independent calculations of the density and bulk modulus of the amorphous multicomponent compound $Zr_{52.5}Cu_{17.9}Ni_{14.6}Al_{10}Ti_5$. This compound forms a glass when it is cooled rapidly and is experimentally well documented. We used 150 atom supercells and the procedure to produce the amorphous structures was the same as before. These two runs are two independent amorphous structures that correspond to two different energy valleys in the PEL.

In both runs, we produced a starting configuration with an average atomic volume of 18.5 Å^3/atom. Then we relaxed the positions of that configuration until convergence using a standard conjugate gradient method. From this relaxed structure, we then constructed two new supercells, one with larger volume and the other with smaller volume by keeping the fractional coordinates of the atoms but rescaling the cell sizes. The atom positions in the new supercells were relaxed in order to obtain the total energy per atom for the new volumes. Then, from the new structures we built subsequent supercells in the same way to cover all volumes. In this way we completed a set of 5 (run 1) and 7 (run 2) data points that are displayed in Fig. 5. The equilibrium density and bulk moduli are shown in Table I. The bulk modulus was obtained by fitting the data points to a modified Morse function.[31]

TABLE I. Calculated and experimental bulk moduli and equilibrium average atomic volumes of the two runs on amorphous $Zr_{52.5}Cu_{17.9}Ni_{14.6}Al_{10}Ti_5$.

	V (Å^3/atom)	V_{exp} (Å^3/atom)	B (GPa)	B_{exp} (GPa)
Run 1	18.44	17.94[a]	103.47	114[a]
Run 2	18.42	17.94[a]	113.20	114[a]

[a]Reference 30.

The results are in excellent agreement with experiments for both the average atomic volume and bulk modulus. The difference between the runs is less than 10% even though we used the relatively small cell size of 150 atoms to describe the alloy. Based on the discussion around Fig. 1 and our results for Al, V, and Vitreloy (105) we speculate that the sharp peak in the potential-energy minima distribution is not a feature that is unique to Na, but is common to all metallic glasses. We also argue that it is not until the system size is over 150 atoms that a complex amorphous structure is adequately described.

Our good agreement with experiments confirms findings by others that structural properties of metallic glasses seem to be independent of the cooling rate in the calculation.[10] We believe that this may be understood as an effect from the strong dominance of local energy minima corresponding to amorphous structures in the PEL of metallic materials and the fact that all calculations represent ultrafast cooling compared to the experimental time scales. Therefore our stochastic quenching procedure for finding amorphous structures may be applied to a wide span of technologically important materials.

IV. CONCLUSIONS

We have performed a statistical analysis of the distribution of local energy minima for a monatomic Na using two different pair potentials. In both cases, the system size was varied from 1 to 4000 atoms and for systems with more than 150 atoms the appearance of a sharp peak was observed in the distributions. The mean of this peak as well as the mean of the total distribution converge to an asymptotic value at above 150 atoms system size. The standard deviations of the distributions converge to zero as the system size increases. This analysis indicates that at around a system size of 150 atoms the thermodynamic limits for Na is reached, where the random valleys dominate the potential-energy landscape.

We performed first-principles calculations of the total energy as function of system size for amorphous Al and V and found that the asymptotic value may be reached at about the same system sizes as for Na. The efficiency of the stochastic quench method and the validity of our system size limit were shown by calculations of the bulk modulus and density of the bulk metallic glass $Zr_{52.5}Cu_{17.9}Ni_{14.6}Al_{10}Ti_5$ (Vitreloy 105) by means of two separate 150 atom supercells and the results agree well with experiments.

The analysis presented here shows that it is essential to perform calculations of system sizes that describe the thermodynamic limit correctly to properly characterize metallic liquids and metallic glasses. We hence conclude that performing averages over many small systems cannot improve the accuracy of calculations since many symmetric structures will be included. These structures do not belong to the sharp peak of the distribution of local minima and therefore to include them in an average may result in severe errors.

The stochastic quenching is a method that ensures a high probability of finding an amorphous structure with a low computational cost. We believe that this method opens up an efficient and computationally reasonable way for theoretical

discovery of new complex amorphous materials by means of first-principles DFT methods.

ACKNOWLEDGMENTS

E.H. would like to thank for support by FONDECYT under Grant No. 11070115. R.L. was supported by FONDECYT under Grant No. 11080259. The Los Alamos National Laboratory is operated by Los Alamos National Security, LLC for the NNSA of the U.S. DOE under Contract No. DE-AC52-06NA25396.

[1] W. Johnson, JOM **54**, 40 (2002).
[2] A. Inoue, Acta Mater. **48**, 279 (2000).
[3] A. Inoue, B. Shen, and N. Nishiyama, *Bulk Metallic Glasses* (Springer, New York, 2007).
[4] A. Inoue and X. Wang, Acta Mater. **48**, 1383 (2000).
[5] S. J. Pang, T. Zhang, K. Asami, and A. Inoue, Acta Mater. **50**, 489 (2002).
[6] V. Ponnambalam, S. J. Poon, G. J. Shiflet, V. M. Keppens, R. Taylor, and G. Petculescu, Appl. Phys. Lett. **83**, 1131 (2003).
[7] T. D. Shen and R. B. Schwarz, Appl. Phys. Lett. **75**, 49 (1999).
[8] P. Hohenberg and W. Kohn, Phys. Rev. **136**, B864 (1964).
[9] W. Kohn and L. Sham, Phys. Rev. **140**, A1133 (1965).
[10] H. W. Sheng, W. K. Luo, F. M. Alamgir, J. M. Bai, and E. Ma, Nature (London) **439**, 419 (2006).
[11] G. Gutiérrez and B. Johansson, Phys. Rev. B **65**, 104202 (2002).
[12] E. Holmström, N. Bock, T. B. Peery, R. Lizárraga, G. De Lorenzi-Venneri, E. D. Chisolm, and D. C. Wallace, Phys. Rev. E **80**, 051111 (2009).
[13] D. C. Wallace, Phys. Rev. E **56**, 4179 (1997).
[14] G. De Lorenzi-Venneri and D. C. Wallace, Phys. Rev. E **76**, 041203 (2007).
[15] C. Chakravarty, P. G. Debenedetti, and F. H. Stillinger, J. Chem. Phys. **123**, 206101 (2005).
[16] P. E. Blöchl, Phys. Rev. B **50**, 17953 (1994).
[17] G. Kresse and D. Joubert, Phys. Rev. B **59**, 1758 (1999).
[18] G. Kresse and J. Hafner, Phys. Rev. B **47**, 558 (1993).
[19] G. Kresse and J. Hafner, Phys. Rev. B **49**, 14251 (1994).
[20] G. Kresse and J. Furthmüller, Phys. Rev. B **54**, 11169 (1996).
[21] G. Kresse and J. Furthmüller, Comput. Mater. Sci. **6**, 15 (1996).
[22] J. P. Perdew, K. Burke, and M. Ernzerhof, Phys. Rev. Lett. **77**, 3865 (1996).
[23] D. C. Wallace, Phys. Rev. **176**, 832 (1968).
[24] D. C. Wallace and B. E. Clements, Phys. Rev. E **59**, 2942 (1999).
[25] D. C. Wallace, *Statistical Physics of Crystals and Liquids* (World Scientific, New Jersey, 2002).
[26] W. Kob, J. Phys.: Condens. Matter **11**, R85 (1999).
[27] F. Sciortino, W. Kob, and P. Tartaglia, Phys. Rev. Lett. **83**, 3214 (1999).
[28] S. Büchner and A. Heuer, Phys. Rev. E **60**, 6507 (1999).
[29] S. Sastry, Nature (London) **409**, 164 (2001).
[30] Z. Bian, M. Xiang Pan, Y. Zhang, and W. Hua Wang, Appl. Phys. Lett. **81**, 4739 (2002).
[31] V. L. Moruzzi, J. F. Janak, and K. Schwarz, Phys. Rev. B **37**, 790 (1988).